nature geoscience

SUPPLEMENTARY INFORMATION

DOI: 10.1038/NGEO1109

Impact of fjord dynamics and glacial runoff on the circulation near Helheim Glacier

1. Circulation and Heat Transport in the proximity of Helheim Glacier

Direct velocity measurements were obtained in summer 2009 at all CTD stations using a lowered Acoustic Doppler Current Profiler (lADCP, an RDI 300 kHz). Six of these were obtained at sections 7 and 6, within 20 km of Helheim's front, Fig 1. Two additional temperature and velocity profiles were obtained from expendable current profilers (XCP) closer to the front, Fig 1. Of the two, only one had velocity errors that were small compared to the observed flows (the errors were likely due to interference of the radio signal with the ice in the fjord). Each profile was corrected for the magnetic declination by using the declination from NOAA's National Geophysics Data Center http://www.ngdc.noaa.gov) at the time when the profile was collected. The velocities were then rotated into an along and across component for the principal axis of the left arm of Sermilik Fjord, known as Helheim Fjord. In general, the along-fjord velocity was only slightly larger than the across. The along-fjord velocities for the profiles in the vicinity of Helheim Glaciers are shown in Supplementary Figure 1 together with the potential density profiles from the corresponding CTD data.

The data reveal fast, strongly sheared flows which typically reverse at the PW/STW interface, where the CTD profiles show a large change in stratification. Profiles within each section, taken a few hours apart, resemble each other but profiles from section 6 are roughly of the opposite sign from those at section 7, occupied roughly 24 hours later. The XCP velocity profile collected approximately 6 hours prior to the occupation of section 7 has a flow structure that resembles that of the profiles from section 6. These observations suggest that flows reverse over periods of hours. The similarity in structure for all profiles (including the reversal of the flow at the PW/STW interface) and their temporal variability suggest that the instantaneous profiles are dominated by intermediary circulations[14], internal seiches[20] or internal waves[17] of the fjord excited by external forcing (e.g. wind) or by glacial processes. The vertical displacement associated with these modes is less than ~50m as shown, for example, in moored data from the fjord[14], and consistent with the variability observed during the occupation of a section (6-12 hours). Thus, we expect the property variability associated with the seiches to be much less than the anomalies shown in Figure 3.

The oscillatory nature of the instantaneous flows indicates that they are not representative of the net circulation transporting heat to the ice-edge, though they likely play a role in it. We show this by estimating the heat transport associated with each profile. Because we were unable to collect data across the entire width of the fjord, due to ice, we treat each profile separately and assume it is representative of the entire fjord's width (4 km). All velocity profiles extend to the bottom. Since the heat transport is also highly sensitive to any net mass flux, we compute heat transport in two ways: from the observed profile data and from the profile data corrected, by adding a barotropic (uniform with depth) velocity component, specific to each profile, that forces the vertically integrated mass transport for each profile to be zero. For all profiles the barotropic velocity correction was small (order 1 cm/s) and its sign varied. The heat transport estimate for each profile (using both the corrected and the uncorrected velocity) is shown in Supplementary Figure 1c. These calculations clearly involve large uncertainties but they do show that the observed flow reversals cause reversals in the sign of the transport

DOI: 10.1038/NGEO1109

of heat. The sign reversals of the heat transport are simply due to the fact that, during the occupation of section 7, the STW layer was mostly flowing towards the glacier and the PW away from it, thus transporting heat to the glacier, while the reversed flows transported heat away from the glacier during the occupation of section 6 and the XCP profile. To convert the heat transport to a melt rate, we estimate that 1 TW (10^{12} W) will melt approximately 95 km^3/yr, assuming a latent heat of fusion of 334500 J/kg, a specific heat capacity of sea water of 3980 J/(kg K), a density of ice of 930 kg/m^3, an initial ice temperature of -10 °C and specific ice capacity of 2100 J/(kg K).

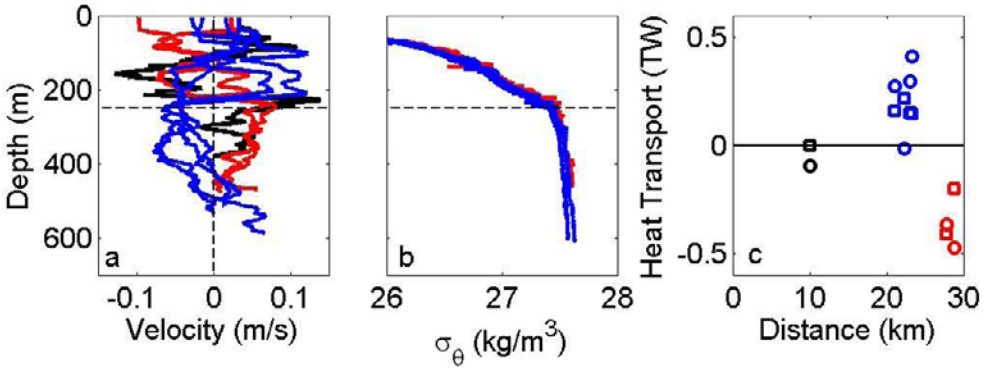

Supplementary Figure 1: Instantaneous Circulation and Heat Transport near Helheim. a) Along-fjord velocity profiles in the vicinity of Helheim's front from section 7 (blue), 6 (red) and from the single XCP which returned data (black). Positive indicates flow away from the glacier (see Fig 1 for station location). b) Potential density profiles for the profiles from sections 6 and 7. The upper limit of the STW layer, ~250 m, is indicated by a dashed line. c) Heat transport in terawatts estimated from the velocities shown in a) and corresponding temperature profiles, positive means heat transport to the glacier. Circles are for observed velocities, squares for velocities corrected to conserve mass.

2. Property Transformation as a result of glacial melt and run-off.

i. Slope of the meltwater mixing line

Melting of ice lowers both the temperature and salinity of the ambient water. If the ice-ocean system is closed and the ambient water is homogeneous, then the potential temperature/salinity (θ/S) characteristics of the ambient/meltwater mixture will fall along a straight *meltwater line*[21] in θ/S space, that joins the ambient water's θ/S properties with the ice's θ_{eff}/S, where θ_{eff} is the effective potential temperature of the ice which takes into account that heat is needed to melt ice, and is given by Equation (2) of Jenkins (1999)[22]:

$$\theta eff = \theta f - \frac{L}{Cp} - \frac{Ci}{Cp}(\theta f - \theta i)$$

where θ_f is the freezing point temperature of water (which depends on salinity and pressure), L is the latent heat of fusion for ice, θ_i is the actual ice temperature, Ci and Cp are the specific heat capacities of ice and water respectively. If the ambient waters are non-homogeneous but their θ/S characteristics fall on a straight line, then the θ/S properties of the meltwater mixture will fall within a triangle defined by the meltwater lines characteristic of the two extreme water masses (again if glacial melt is the only process modifying the waters)[22].

This second situation applies to Sermilik Fjord where the ambient water consists of a mixture of STW and PW and whose θ/S characteristics fall along the line connecting the θ/S characteristics of the two waters (see mouth profiles in Figure 4a and f). In summer, the characteristic θ/S slope of the ambient water (Supplementary Table 1) is roughly equivalent to the slope for the meltwater line estimated according to Jenkins (1999) using an approximate column-averaged ice temperature of -10 °C [cf. Iken et al (1993)[25] for Jakobshavn Glacier in West Greenland], a latent heat of fusion of 334500 J/kg, a specific heat capacity of ice (sea water) of 2100 (3980) J/(kg K) and freezing point temperature of -1.5 °C. (Note that the meltwater line slope obtained, 2.8 °C/psu, is not very sensitive to the values of the ice temperature or freezing point temperature chosen.) The similarity of these slopes implies that the predicted triangle reduces to a single line and, furthermore, that the θ/S characteristics of the ambient/meltwater mixture will tend to fall on the same line as those of the ambient waters. In winter, the θ/S slope of the ambient waters is not as close as that of the predicted meltwater mixing line, implying that one might expect to see the meltwater mixture depart from the ambient line.

Supplementary Table 1 – STW and PW water characteristics

	S – STW (psu)	θ – STW (°C)	σ_θ –STW (kg/m^3)	S – PW (psu)	θ – PW (°C)	σ_θ –PW (kg/m^3)	θ/S slope ambient (°C/psu)
August	34.70	3.4	27.6	33.5	-0.25	26.9	3.04
March	34.75	4.5	27.55	32.9	-1.6	26.5	3.3

ii. Melting plus run-off

Similarly to submarine melt, the addition of run-off to ambient water with certain θ/S characteristic will fall along a mixing line whose endpoints are the θ/S of the pure ambient water and θ=0 °C, S=0 (i.e. fresh water at freezing temperature). An example of such a run-off line for ambient waters at 300 m is shown in Figure 4a-e. The slope of this 'run-off' line tends to be smaller than that associated with submarine melt since for water temperatures characteristic of the polar regions, mixing with run-off has a smaller effect on temperature than melting ice. The run-off line shown in Figure 4a-e, for example, has a slope of 0.07 °C/psu. (We note that allowing for supercooling of the subglacial run-off will tend steepen this gradient but that it will still be much less than the mixing line gradient). A mixture of ambient water, meltwater and run-off, then, will have properties which, in θ/S space, fall somewhere in between the run-off and the meltwater lines. This is the case for the waters above ~270 m in the proximity of Helheim Glacier, Fig 4a-e, whose θ/S characteristics are indicative of a slope of 1.1 °C/psu, i.e. a value in between the expected meltwater and run-off line, Figure 4a-e.

3. Density of the meltwater/ambient water mixture

The meltwater content of an ambient water/meltwater mixture is limited by the amount of heat available to melt the ice (in the ambient water) and amounts to approximately (θ_w-

DOI: 10.1038/NGEO1109

θ_f) % ($^oC^{-1}$) where θ_w is the temperature of the ambient water and θ_f is the freezing temperature of water with the same salinity as the ambient water and at a certain pressure. Given the winter STW properties of (θ_w ~ 4.5 °C, S~34.75), and a pressure of 500 dbars, then the maximum meltwater fraction is 7% (see equation [7] in Jenkins (1999)), and this mixture would have a salinity of 32.33. Doubling of the volume due to entrainment of STW would result in water with salinity of 33.5 and a density that is larger than that of PW. If we consider the problem as a two-dimensional line plume rising vertically through a homogeneous non-rotating environment, we expect[26] doubling of the volume, or equivalent the density of the rising fluid to exceed that of the PW, within tens of meters given an upper estimate of the melt rate of 50 km^3/yr (although the solution is only weakly sensitive to this number).

Additional References

25. Iken, A., Echelmeyer, K., Harrison, W. D., and Funk, M. Mechanisms of fast flow in Jakobshavn Isbrae, Greenland, Part I: Measurements of temperature and water level in deep boreholes. J. of Glaciology, 39, 15-25 (1993).

26. Turner, J. S. *Buoyancy Effects in Fluids*. Cambridge University Press (1973).